ELSEVIER

Pattern Recognition Letters 20 (1999) 229–240

Pattern Recognition Letters

Bayesian detection of the fovea in eye fundus angiographies [1]

M.V. Ibañez, A. Simó *

Dpto. de Matemáticas, Univ. Jaume I, Campus de Penyeta Roja, 12071 Castellón, Spain

Received 3 August 1998; received in revised form 27 October 1998

Abstract

This paper is concerned with the automatic detection of the avascular foveal zone (fovea), in eye fundus angiographies. Fluorescein angiography is used in ophthalmic practice to evaluate vascular retinopathies and choroidopathies: sodium fluorescein is injected in the arm's cubital vein of the patient and its distribution along retinal vessels at certain times is observed. The proposed methodology is based on Bayesian statistical methods that allow to incorporate the previous knowledge about the eye fundus in the model. The contour of the fovea is modeled by means of a unidimensional Markov chain and the observed intensities are assumed Gaussian and statistically independent between pixels. Two approximations are used in order to estimate the model's parameters: Empirical and Fully Bayesian. Two algorithms have been used in order to estimate the fovea contour: Simulated Annealing (SA) and Iterated Conditional Modes (ICM). This procedure is applied to different cases of diabetic retinopathy and vein occlusions.

Keywords: Random field models; Bayesian image analysis; MCMC methods; Fundus eye angiography

1. Introduction

The use of computer based image analysis systems has opened a new investigation way in medical practice, and it has promoted the interest in automatic image analysis as a powerful diagnostic tool. These computer techniques provide useful tools in order to manipulate and quantify features of interest in the image we are going to analyze.

This work is only a part of a more extensive study about automatic detection of two ocular diseases: diabetic retinopathy and vein occlusion. They are the commonest cause of blindness in the working-age population in developed countries. A previous work of one of the authors is (Domingo et al., 1997). The purpose of the present work is to develop and to implement an automatic detection method of the avascular foveal zone (fovea). The fovea is the most accuracy vision zone of the retina, so the nearer the fovea are the graver the ocular lesions are. For this reason, the determination of the fovea is a necessary first step in any study of ocular diseases.

* Corresponding author. E-mail: simo@mat.uji.es

[1] Electronic Annexes available. See http://www.elsevier.nl/locate/patrec.

0167-8655/99/$ – see front matter
PII: S0167-8655(98)00137-8

We are going to work with series of ocular fundus images which have been digitized and stored. They have been obtained by means of fluorescein angiography. This technique consists of an injection of sodium fluorescein in the arm's cubital vein followed by observation of its distribution along retinal vessels at certain times. It provides the ability of vein and cavities visualization, and the possibility of existent diseases detection.

Previous works about segmentation of ocular fundus images are: Chaudhuri et al. (1989) who proposed the design of specific filters matched for the segmentation of ocular fundus images; Liu and Sun (1993) who work in the blood vessels segmentation, and suggesting an algorithm based on a tracking procedure under a Detection–Deletion scheme; and Kutka and Stier (1996) who used for the extraction of blood vessels a tracking algorithm which takes into account line properties.

In this paper we regard the segmentation task as a statistical parameter estimation problem, considering the observed image Y as a noisy version of the true image, X. So, we suppose that X is a parameter of Y's distribution and our goal will be its estimation. The image processing algorithms are better if they are based on mathematical models, and usually in medical images we have a priori knowledge about the features and structures we are looking for. Consequently, Stochastic Models and Bayesian Statistical theory will be very useful tools for us.

1.1. Markov random fields

Markov Random Fields (Cressie, 1993) allow the definition of probability distributions on a set of dependent variables.

If we assume every digitized image is stored as a finite regular lattice with sites labeled by integer pairs (i,j), and we identify every image pixel with a lattice site, associated to the lattice sites we have a set of random variables $\{X(i,j)\}$. Every $X(i,j)$ has information about the grey level in the pixel (i,j). Therefore, a digitized image can be regarded as a Markov Random Field (MRF) on a lattice with a finite state space.

The MRF model will incorporate the dependence between neighboring pixels and it will give high probabilities to images whose features are similar to those we are looking for.

The most useful and easy way to specify the probability distribution of an MRF is writing it in terms of a Gibbs distribution which is the sum of a set of local potential functions

$$\Pi(\{X(i,j)\}) \propto \exp\left\{ -\sum_{C\in\mathscr{C}} V_C(\{X(i,j)\colon (i,j)\in C\})\right\}, \tag{1}$$

where $\mathscr{C}$ is the set of all cliques associated to a given neighborhood system, and a clique is any set of either with only one site or else with mutually neighbor sites.

1.2. Bayesian image analysis

Bayesian methods have been largely used in medical image analysis, such as the reconstruction from single-photon emissions computed tomography data (Geman and McClure, 1987; Aykroyd and Green, 1991; Green, 1990; Weir and Green, 1994; Weir, 1997).

In a Bayesian framework we assume that associated to the lattices sites, we have $Y = \{Y(i,j) : (i,j)\in S\}$ observed image, and $X = \{X(i,j)\colon (i,j)\in S\}$ true image, S being the set of lattice sites.

To correctly model the observed image, the noise has to be taken into account. If we suppose only the presence of additive noise,

$$Y = X + \epsilon.$$

We will have:
- $f(Y/X)$ observed image distribution given the true image.
- $\pi(X)$ a priori true image distribution.

In order to estimate the true image, we look for

$$\max\ f(X/Y).$$

And according to Bayes law,

$$f(X/Y) = \frac{f(Y/X)\pi(X)}{f(Y)},$$

so we will take the maximum of the posteriori probability given the observed image, i.e.,

$$\hat{X} = \arg\ \max\{f(Y/X)\pi(X)\}.$$

Basic references of Bayesian Image Analysis are: Besag (1986), Geman and Geman (1984), Cressie (1993), Guyon (1995) and Winkler (1996).

Due to the complexity of the statistical distributions we found, analytical parameter estimation methods will be inadequate. So we will use several estimation specific algorithms, like the "Iterated Conditional Modes" (ICM) or "Simulated Annealing" (SA).

For the sake of analytical and computational simplicity we use a polar coordinate system: (ρ, θ) where $\rho \in \Lambda$, and $\theta \in [0, 2\pi]$. So we will describe the fovea's contour by an one-dimensional MRF, and we will work only with n directions: $\theta \in \{\theta_1, \ldots, \theta_n\}$.

The paper is organized as follows. In the next section the model of the observed data is introduced. The prior distribution of the fovea's contour is given in Section 3. Section 4 deals with parameter estimation. In Section 5 we describe the estimation algorithm and its implementation, and finally, Section 6 shows the results of applying our methodology to some digital angiographies.

2. Modeling the observed image

In this section we describe the image generation mechanism, but first, we introduce a new coordinate system.

2.1. Coordinate system

Looking for analytical and computational simplicity we use a polar coordinate system, (ρ, θ) where $\rho \in \Lambda$ and $\theta \in [0, 2\pi]$. So, we describe the fovea's contour by a one-dimensional MRF, and we work only with n directions $\theta \in \{\theta_1, \ldots, \theta_n\}$, and L pixels on each direction, where $L = |\Lambda|$.

The center of the coordinate system is taken manually, and n directions are chosen.

Once we have all the image expressed in the same coordinate system:
- $Y = \{Y(\theta_i, \rho) : i \in 1, \ldots, n, \rho \in \Lambda\}$ observed image.
- $X = \{X(\theta_i, \rho) : i \in 1, \ldots, n, \rho \in \Lambda\}$ true image.
- $r = \{r_i = r(\theta_i); i = 1, 2, \ldots, n\}$ fovea contour.

2.2. Likelihood function

The fovea is an avascular eye zone, so inside and outside its contour it will have different grey levels. So we suppose

$$X(\theta_i,\rho,r_i)=\begin{cases}A_i & \text{if } \rho<r_i,\\ C_i & \text{if } \rho\geqslant r_i,\end{cases}$$

A_i and C_i being inside and outside (respectively) fovea contour grey intensities.

To model the observed image, noise has to be taken into account. If we suppose the image has been affected by additive white Gaussian noise only,

$$Y(\theta_i,\rho,r_i)=\begin{cases}X(\theta_i,\rho,r_i)+n_{A_i} & \text{if } \rho<r_i \text{ with } n_{A_i}\sim N(0,\sigma^2_{A_i}),\\ X(\theta_i,\rho,r_i)+n_{C_i} & \text{if } \rho\geqslant r_i \text{ with } n_{C_i}\sim N(0,\sigma^2_{C_i}),\end{cases}$$

and simplifying notation, we define $X_i=(X(\theta_i,1,r_i),X(\theta_i,2,r_i),\ldots,X(\theta_i,L,r_i))^{\mathrm{T}}$, $Y_i=(Y(\theta_i,1,r_i),Y(\theta_i,2,r_i),\ldots,Y(\theta_i,L,r_i))^{\mathrm{T}}=(y_i(1),y_i(2),\ldots,y_i(L))^{\mathrm{T}}$, then the likelihood function is found to be

$$f(Y_i/A_i,C_i,r_i)=\frac{1}{\sqrt{(2\pi)^L}\sigma^{r_i}_{A_i}\sigma^{L-r_i}_{C_i}}\exp\left\{-\frac{1}{2}(X_i-Y_i)'Q^{-1}(X_i-Y_i)\right\},$$

so

$$f(Y_i/A_i,C_i,r_i)\propto\exp\left\{-\frac{1}{2}\left[r_i\left(\frac{A_i^2}{\sigma^2_{A_i}}-\frac{C_i^2}{\sigma^2_{C_i}}\right)+\left(\frac{1}{\sigma^2_{A_i}}\sum_{j=1}^{r_i}y_i^2(j)-2A_i\sum_{j=1}^{r_i}y_i(j)\right)\right.\right.$$
$$\left.\left.+\frac{1}{\sigma^2_{C_i}}\left(LC_i^2+\sum_{j=r_i+1}^{L}y_i^2(j)-2C_i\sum_{j=r_i+1}^{L}y_i(j)\right)\right]\right\}. \tag{2}$$

3. A priori probability

The a priori distribution of the fovea's contour is modeled by means of a unidimensional MRF. We use a first order neighborhood system. Cliques associated with this neighborhood system are

1. $C_i^{(1)}=\{r_i\}$,
2. $C_i^{(2)}=\{r_i,r_{i-1}\}$.

The consulted ophthalmologist affirms that the fovea's contour has, with high probability, a circular or elliptical shape. So, we penalize improbable configurations which are characterized by neighbor module differences. Then

- $V_{C_i^{(1)}}=0$,
- $V_{C_i^{(2)}}=\lambda^2(r_i-r_{i-1})^2$,

where λ is a constant. So,

$$\pi(r_i/r_j\in\delta_i)\propto\exp\left\{-\lambda^2\left[(r_i-r_{i-1})^2+(r_{i+1}-r_i)^2\right]\right\},$$

δ_i being the set of neighbor sites of pixel i. And finally

$$\pi(r_i/r_j\in\delta_i)\propto\exp\left\{-2\lambda^2\left(r_i-\frac{r_{i-1}+r_{i+1}}{2}\right)^2\right\}. \tag{3}$$

Then, the a priori probability has the expression

$$\pi(r) \propto \exp \sum_{i=1}^{n} \left\{ \frac{-\lambda^2}{2} (2r_i - r_{i-1} - r_{i+1})^2 \right\}. \tag{4}$$

According to Bayes law,

$$\hat{r}_{\mathrm{MAP}} = \arg \max_r \{f(r/Y)\} = \arg \max_r \{f(Y/r)\pi(r)\}. \tag{5}$$

So, with Eqs. (2), (4) and (5) we have

$$f(r/Y) \propto \exp \frac{-1}{2} \sum_{i=1}^{n} \left\{ \frac{1}{\sigma_{A_i}^2} \left(A_i^2 r_i + \sum_{j=1}^{r_i} \left(y_i^2(j) - 2A_i y_i(j) \right) \right) \right.$$
$$\left. - \frac{1}{\sigma_{C_i}^2} \left(r_i C_i^2 + \sum_{j=r_i+1}^{L} \left(2C_i y_i(j) - y_i^2(j) \right) \right) + \lambda^2 (2r_i - r_{i-1} - r_{i+1})^2 \right\}. \tag{6}$$

3.1. Conditional probability

The optimization algorithms we use (ICM and SA) need the conditional probability distribution function, because they optimize the conditional distribution of every pixel, given the rest.

The conditional distribution expression is found to be

$$f(r_i/r_j : j \neq i, Y) \propto \exp \frac{-1}{2} \left\{ \frac{1}{\sigma_{A_i}^2} \left(A_i^2 r_i + \sum_{j=1}^{r_i} \left(y_i^2(j) - 2A_i y_i(j) \right) \right) \right.$$
$$\left. - \frac{1}{\sigma_{C_i}^2} \left(r_i C_i^2 + \sum_{j=r_i+1}^{L} \left(2C_i y_i(j) - y_i^2(j) \right) \right) + \lambda^2 (2r_i - r_{i-1} - r_{i+1})^2 \right\}$$

Once we have the observed image modeled, the optimization is carried out in this work by two different methods: ICM and SA.

These methods need also an initial fovea contour estimation. We choose the maximum likelihood estimator because it provides a good initial estimate without expensive computational cost.

4. Parameter estimation

The model has a set of unknown parameters which have to be estimated. Two different estimation methods are used: Fully Bayesian Estimation and Empirical Bayesian Estimation.

4.1. Empirical Bayesian estimation

In the Empirical Bayesian Estimation, we suppose parameters are unknown but fixed. If we would know r, the estimation task would be done using

$$\widehat{A}_i = \frac{1}{r_i}\sum_{j=1}^{r_i} y_i(j), \tag{7}$$

$$\widehat{C}_i = \frac{1}{L-r_i}\sum_{j=r_i+1}^{L} y_i(j), \tag{8}$$

$$\widehat{\sigma^2_{A_i}} = \frac{1}{r_i}\sum_{j=1}^{r_i}\left(y_i(j) - \widehat{A}_i\right)^2, \tag{9}$$

$$\widehat{\sigma^2_{C_i}} = \frac{1}{L-r_i}\sum_{j=r_i+1}^{L}\left(y_i(j) - \widehat{C}_i\right)^2. \tag{10}$$

However, r is one of the parameters we want to estimate. So, in each algorithm step, we are going to update $\widehat{A}_i$, $\widehat{C}_i$, $\widehat{\sigma^2_{A_i}}$ and $\widehat{\sigma^2_{C_i}}$ according to previous expressions, using the previous estimated r_i values.

4.2. Fully Bayesian Estimation

In Fully Bayesian Estimation, the parameters are considered random variables with a given probability distribution.

This procedure was used in Johnson (1994), Mollie (1996), Weir (1997) and Molina (1994), because the models (likelihood and a priori) they found, were not a correct description of the processes.

We use Fully Bayesian Estimation to estimate A_i and C_i.

We know that the fovea is an avascular zone, thus it will become darker in its central part. We have a prior knowledge about A_i but we do not know anything about C_i (outside the fovea's contour we have dark pixels belonging to the background and bright pixels, belonging to veins and arteries). So we suppose both have a Gaussian multivariate distribution with fixed parameters:

$$\pi(A_1,\ldots,A_n) = \frac{1}{\left(2\pi\tilde{\sigma}^2_{A_i}\right)^{n/2}}\exp\left(-\frac{1}{2\tilde{\sigma}^2_{A_i}}\sum_{i=1}^{n}\left(A_i-\mu_{A_i}\right)^2\right), \tag{11}$$

$$\pi(C_1,\ldots,C_n) = \frac{1}{\left(2\pi\tilde{\sigma}^2_{C_i}\right)^{n/2}}\exp\left(-\frac{1}{2\tilde{\sigma}^2_{C_i}}\sum_{i=1}^{n}\left(C_i-\mu_{C_i}\right)^2\right). \tag{12}$$

The mean of Eq. (11) will be small, and that of Eq. (12) will be large. Variance will be larger in Eq. (12) than in Eq. (11) because inside the fovea's contour we have a more uniform dark zone, while outside we have pixels belonging to veins and arteries, and pixels belonging to the background.

Then

$$f(r,A_i,C_i/Y)\alpha f(Y/r,A_i,C_i)\pi(r)P(A_i,C_i)$$

$$\propto\prod_{i=1}^{n}\left[\exp\left\{-\frac{1}{2}\left[\frac{1}{\sigma^2_{A_i}}\left(r_iA_i^2 - 2A_i\sum_{j=1}^{r_i}y_i(j) + \sum_{j=1}^{r_i}y_i^2(j)\right)\right.\right.\right.$$

$$+\frac{1}{\sigma_{C_i}^2}\left((L-r_i)C_i^2-2C_i\sum_{j=r_i+1}^{L}y_i(j)+\sum_{j=r_i+1}^{L}y_i^2(j)\right)+4k^2\left(r_i-\frac{r_{i-1}+r_{i+1}}{2}\right)^2\Bigg]$$

$$+\left(-\frac{1}{2\tilde{\sigma}_{A_i}^2}\left(A_i-\mu_{A_i}\right)^2\right)+\left(-\frac{1}{2\tilde{\sigma}_{C_i}^2}\left(C_i-\mu_{C_i}\right)^2\right)\Bigg\}\Bigg].$$

So, A_i and C_i parameter estimators will be

$$\widehat{A}_i=\frac{\tilde{\sigma}_{A_i}^2\sum_{j=1}^{r_i}y_i(j)+\hat{\sigma}_{A_i}^2\mu_{A_i}}{\tilde{\sigma}_{A_i}^2 r_i+\hat{\sigma}_{A_i}^2}, \tag{13}$$

$$\widehat{C}_i=\frac{1}{\tilde{\sigma}_{C_i}^2(L-r_i)+\hat{\sigma}_{C_i}^2}\left(\hat{\sigma}_{C_i}^2\mu_{C_i}+\tilde{\sigma}_{C_i}^2\sum_{j=r_i+1}^{L}y_i(j)\right). \tag{14}$$

Once the parameters are initialized, we use some optimization method which performs simultaneous parameter and contour estimation.

5. Implementation

A sketch of the estimation algorithm is as follows:

- *Step 0*. Data introduction and initialization.
- *Step 1*. Initial estimation of the fovea's contour delimited points. The initial estimator will be the maximum likelihood one.
- *Step 2*.
  - If ICM algorithm is used, go to 3.
  - If SA algorithm is used, go to 4.
- *Step 3* (*ICM*). For each direction, we compute $f(r_i/r_j: j\neq i, Y)$ for each r_i. We take the point which minimizes its conditional distribution given the rest.
  Go to 5.
- *Step 4* (*SA*). The cooling schedule is

  $$T(k)=\frac{1}{1.01^k}.$$

  T is called temperature, and it is gradually lowered when the iteration number increases. So the SA algorithm guarantees the convergence to the global maxima of the posteriori distribution. For each iteration and for each direction we choose at random a new r_i with probability

  $$f_T(r_i)\propto\exp\left\{\frac{1}{T(k)}\ln\left(f(r_i/r_j: j\neq i, Y)\right)\right\}.$$

  It is obtained as follows. For each iteration and for each direction we choose a value, k, which

  $$f_T(k)<u<f_T(k+1),$$

  u being a uniform random number between 0 and 1.

Go to 5.

- *Step 5* (*Stopping condition*). The algorithm stops when between two consecutive iterations there is no change in the obtained contour estimation, or when a given number of iterations is reached.
  - If stopping condition is verified, STOP.
  - If stopping condition is not verified, go to 6.
- *Step 6* (*Parameter Actualization*). New parameter estimated values are computed using the updated r_i.
  - If we use Empirical Bayesian Estimation: Eqs. (7)–(10).
  - If we use Fully Bayesian Estimation: Eqs. (13), (14), (9) and (10).

  Go to 2.

6. Results

The previous algorithm has been applied to several ocular fundus images. All these images have been taken by a Canon CF-60U and Nikon NFC 50 fundus cameras, transformed into video signal with a photo video camera PHV-A7E Sony, and digitized with a Matrox MVP-AT card with 512×380 pixels. The images are taken from patients suffering from different lesions such as diabetic retinopathy and vascular occlusions.

The implementation has been written in the C language. For result visualization, a set of image processing libraries called VISTA, has been used.

Parameters of the a priori distribution have been estimated according to both methods: Empirical Bayesian Estimation, and Fully Bayesian Estimation, and the set of the points which delimited the fovea's contour has been estimated according the two different estimation methods: ICM and SA.

Fig. 1 shows two fluorescein angiographies of two patients suffering from diabetic retinopathy and vein occlusion, respectively, and their corresponding initial fovea contour, obtained using maximum likelihood estimation.

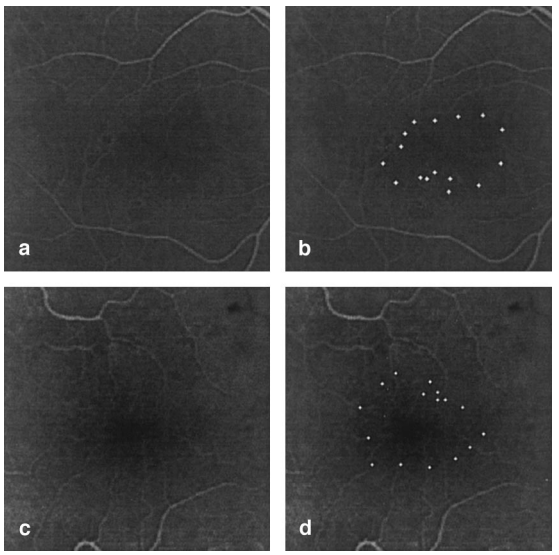

Fig. 1. Two fluorescein angiographies and their initial fovea contour estimation. (a) and (c) show the angiographies from a diabetic retinopathy patient and from a vein oclussion patient, respectively, and their initial fovea contour estimations are in (b) and (d).

In Fig. 2 we see the fovea contour obtained from image (a) of Fig. 1, using the ICM algorithm, for three different values of the parameter λ and using both estimation procedures. Fig. 3 shows similar results from image (b) of Fig. 1. The SA results are shown in Figs. 4 and 5, for the diabetic retinopathy and vein occlusion images, respectively.

The value of parameter λ is critical. High λ values give a large weight to the a priori information. If λ increases, the method used provides a more circular fovea's contour shape.

If we compare the ICM and SA algorithms we can see that both provide good results, with the difference that ICM is faster than SA. ICM reaches convergence in about 6 or 8 iterations, while SA converges in about 600 or 700 iterations. Fig. 6 shows the evolution of the mean grey level estimations against the iteration number, showing the convergence behavior of the algorithm.

The ICM algorithm is more robust than SA with respect to the estimation method used, and the fovea contour obtained is only a little larger than the contour that an ophthalmologist would mark. That is because it responds to the intensity changes introduced in the model.

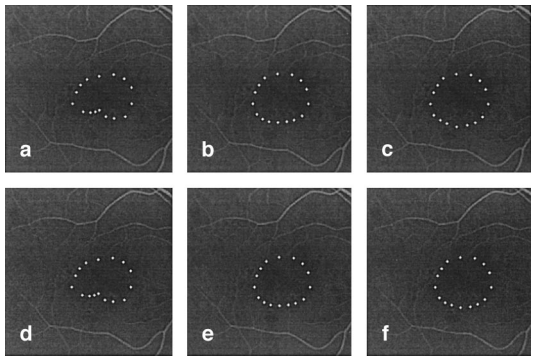

Fig. 2. ICM results from the diabetic retinopathy patient. In (a), (b) and (c) Empirical Bayesian Estimation has been used, meanwhile in (d), (e) and (f) we used Fully Bayesian Estimation. The respective values of λ are (a) $\lambda = 0.1$; (b) $\lambda = 0.8$; (c) $\lambda = 1$; (d) $\lambda = 0.1$; (e) $\lambda = 0.8$; (f) $\lambda = 1$.

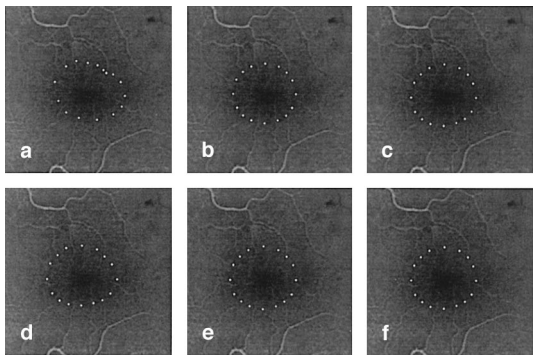

Fig. 3. ICM results from the vein occlusion patient. In (a), (b) and (c) Empirical Bayesian Estimation has been used, meanwhile in (d), (e) and (f) we used Fully Bayesian Estimation. The respective values of λ are (a) $\lambda = 0.1$; (b) $\lambda = 0.8$; (c) $\lambda = 1$; (d) $\lambda = 0.1$; (e) $\lambda = 0.8$; (f) $\lambda = 1$.

SA is slower than ICM, with a higher computational cost, and the result obtained depends more than those obtained with ICM on the value of λ. If λ value increases, the contour of the fovea becomes bigger.

Using Empirical Bayesian Estimation with ICM we obtain similar results to those obtained with SA. On the other hand, with SA, the same λ values provide larger fovea's contours than those obtained using Fully Bayesian Estimation. When the value of λ increases, contours obtained using the Empirical Bayesian Estimation method become larger, while contours obtained using Fully Bayesian Estimation are somewhat smaller, and better according ophthalmologist's opinion.

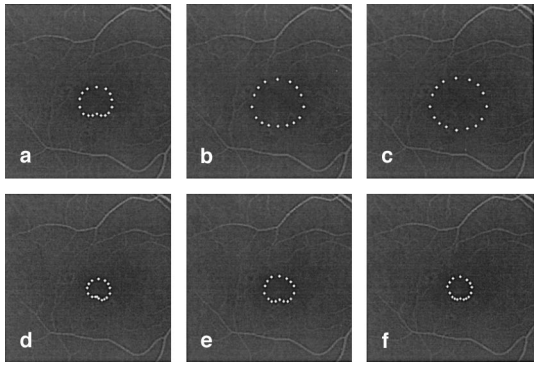

Fig. 4. SA results from the diabetic retinopathy patient. In (a), (b) and (c) Empirical Bayesian Estimation has been used, meanwhile in (d), (e) and (f) we used Fully Bayesian Estimation. The respective values of λ are (a) $\lambda = 0.5$; (b) $\lambda = 0.7$; (c) $\lambda = 0.8$; (d) $\lambda = 0.5$; (e) $\lambda = 0.7$; (f) $\lambda = 0.8$.

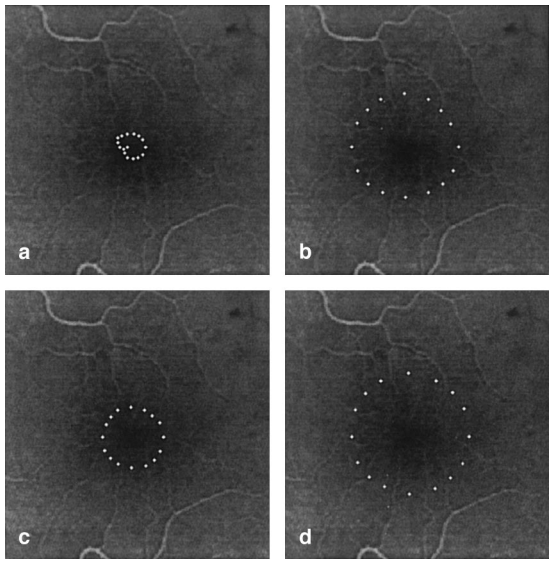

Fig. 5. SA results from the vein occlusion patient. In (a) and (b) Empirical Bayesian Estimation has been used, meanwhile in (c) and (d) we used Fully Bayesian Estimation. The respective values of λ are (a) $\lambda = 0.8$; (b) $\lambda = 1$; (c) $\lambda = 0.8$; (d) $\lambda = 0.1$.

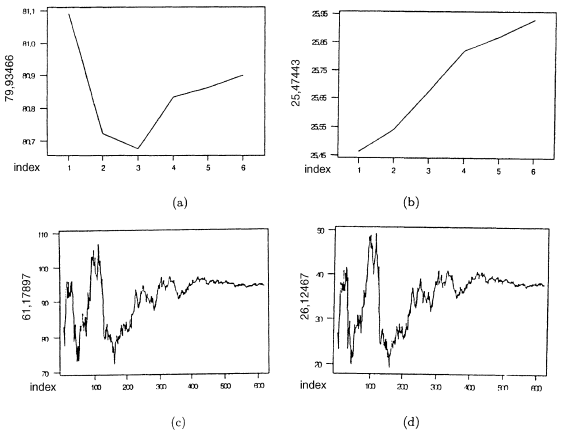

Fig. 6. (a) and (b) show mean intensity estimations using ICM, inside and outside the fovea contour respectively, while in (c) and (d) we have the mean intensities using SA inside and outside the fovea contour.

In conclusion we can say that, in general, we have obtained results that were found quite good by expert clinicians. But, the ICM algorithm is more robust and faster than SA. There is difference between the Fully Bayesian and the Empirical Bayesian Estimation only using SA and in this case the first method provides more realistic fovea contours.

Acknowledgements

We are indebted to Pilar Marco and Lucía Martínez for the eye fundus angiographies.

References

Aykroyd, R.G., Green, P., 1991. Global and local priors, and the location of lesions using gamma-camera imagery. Philos. Trans. R. Soc. London, Ser. A 337, 323–342.

Besag, J., 1986. On the statistical analysis of dirty pictures. J. R. Statist. Soc. B 48, 259–302.

Chaudhuri, S., Chatterjee, S., Katz, M., Nelson, M., Goldbaum, M., 1989. Detection of blood vessels in retinal images using two-dimensional matched filters. IEEE Trans. Medical Imaging 3 (3), 1–5.

Cressie, N., 1993. Statistics for Spatial Data. Wiley Series in Probability and Mathematical Statistics, Wiley, New York.

Domingo, J., Ayala, G., Simó, A., De Ves, E., Martínez-Costa, L., Marco, P., 1997. Irregular motion recovery in fluorescein angiograms. Pattern Recognition Letters 18, 805–821.

Geman, S., Geman, D., 1984. Stochastic relaxation, Gibbs distributions, and the Bayesian restoration of images. IEEE Trans. PAMI 6, 721–741.

Geman, S., McClure, D., 1987. Statistical methods for tomographic image reconstruction. In: Proc. 46th Sess. Inst. Stat. Inst. Bulletin ISI, Vol. 52.

Green, P., 1990. Bayesian reconstruction from emission tomography data using a modified em algorithm. IEEE Trans. Medical Imaging 9, 84–93.

Guyon, X., 1995. Random Fields on a Network. Modeling Statistics and Applications. Springer, Berlin.

Johnson, V., 1994. A model for segmentation and analysis of noisy images. J. Amer. Statist. Assoc. 89, 230–241.

Kutka, R., Stier, S., 1996. Extraction of line properties based on direction fields. IEEE Trans. Medical Imaging 15 (1), 51–58.

Liu, I., Sun, Y., 1993. Recursive tracking of vascular networks in angiograms based on the detection–deletion scheme. IEEE Trans. Medical Imaging 12 (2).

Molina, R., 1994. On the hierarchical bayesian approach to image restoration: applications to astronomical images. IEEE Trans. PAMI 16, 1122–1128.

Mollie, A., 1996. Bayesian mapping of disease. In: Gilks, W., Richardson, S., Spiegelhalter, S. (Eds.), Markov Chain Monte Carlo in Practice, Chapter 20. Chapman & Hall, London.

Weir, I., 1997. Fully bayesian reconstruction from single photon emission computed tomography data. J. Amer. Statist. Assoc. 92 (437), 49–60.

Weir, I., Green, P., 1994. Modeling data from single-photon emission computed tomography. In: Mardia, K. (Ed.), Statistics and Images, pp. 313–338.

Winkler, G., 1996. Image Analysis, Random Fields Models and Dynamic Monte Carlo Methods. Springer, Berlin.